Nanoscale

PAPER

View Article Online
View Journal | View Issue

Cite this: *Nanoscale*, 2015, **7**, 6729

J-aggregation, its impact on excited state dynamics and unique solvent effects on macroscopic assembly of a core-substituted naphthalenediimide†

Haridas Kar,[a] Dominik W. Gehrig,[b] Frédéric Laquai*[b] and Suhrit Ghosh*[a]

Herein we reveal a straightforward supramolecular design for the H-bonding driven J-aggregation of an amine-substituted cNDI in aliphatic hydrocarbons. Transient absorption spectroscopy reveals sub-ps intramolecular electron transfer in isolated NDI molecules in a THF solution followed by a fast recombination process, while a remarkable extension of the excited state lifetime by more than one order of magnitude occurred in methylcyclohexane likely owing to an increased charge-separation as a result of better delocalization of the charge-separated states in J-aggregates. We also describe unique solvent-effects on the macroscopic structure and morphology. While J-aggregation with similar photophysical characteristics was noticed in all the tested aliphatic hydrocarbons, the morphology strongly depends on the "structure" of the solvents. In linear hydrocarbons (*n*-hexane, *n*-octane, *n*-decane or *n*-dodecane), formation of an entangled fibrillar network leads to macroscopic gelation while in cyclic hydrocarbons (methylcyclohexane or cyclohexane) although having a similar polarity, the cNDI exhibits nanoscale spherical particles. These unprecedented solvent effects were rationalized by establishing structure-dependent specific interactions of the solvent molecules with the cNDI which may serve as a general guideline for solvent-induced morphology-control of structurally related self-assembled materials.

Received 22nd January 2015,
Accepted 10th March 2015

DOI: 10.1039/c5nr00483g

www.rsc.org/nanoscale

Introduction

Conjugated π-systems provide diverse opportunities for creating functional supramolecular assemblies[1] with tunable photophysical properties[2] and an enhanced charge-transporting ability[3] as a result of the through space π–π interaction which is of considerable interest in miniaturized organic electronic devices[4] as well as in biological applications.[5] In this context, core-substituted naphthalenediimides (cNDIs)[6] have been explored for a large number of applications[7] including organic solar cells, electron transport in field effect transistors, anion transport, photo-induced electron transport, fluorescence resonance energy transfer, bio-sensing and in donor–acceptor type conjugated polymers[8] owing to their substitution-dependent tunable absorption spanning over almost the entire visible range, their superior fluorescence properties, variable π-acidity and tunable electrochemical properties. Unlike the bay-substituted perylene dyes, the cNDIs retain the planarity of the aromatic ring even after core substitution and thus π-stacking is not hindered. Nevertheless, in contrast to a large number of reports on supramolecular assembly of core unsubstituted NDIs[9–11] such examples on cNDIs are still rare,[12] possibly due to the lack of a facile synthetic route for their preparation until a recent surge in this field.[13] However, even those examples do not adequately elucidate the precise nature of the inter-chromophoric interactions or the impact of self-assembly on photophysical properties. Considering the structural and functional diversities in this class of π-systems, we envisioned that the supramolecular assembly of cNDIs would be worth investigating to examine the effects of structural nuances on self-assembly, morphology, and photophysical properties.[14] Amongst various substituted derivatives, amine-substituted NDIs are particularly interesting because of their fascinating redox properties (both di-cation and di-anion formation are possible) and photo-induced charge-separation.[15] Herein we reveal the first report of J-aggregation[16] of a core-substituted NDI-derivative and unprecedented solvent effects on macroscopic assembly and their excited state dynamics.

[a]*Polymer Science Unit, Indian Association for the Cultivation of Science, 2A & 2B Raja S. C. Mullick Road, Kolkata, India-700032. E-mail: psusg2@iacs.res.in*
[b]*Max Planck Research Group for Organic Optoelectronics, Max Planck Institute for Polymer Research, Ackermannweg 10, D-55128 Mainz, Germany. E-mail: laquai@mpip-mainz.mpg.de*

† Electronic supplementary information (ESI) available: Synthesis and characterization, additional spectroscopic and microscopic data on self-assembly and gelation test details in various solvents. See DOI: 10.1039/C5NR00483G

Results and discussion

H-bonding driven J-aggregation

The structure of the amine-substituted NDI derivative **cNDI-1** is shown in Scheme 1. It was synthesized in a few steps (Scheme S1†) from naphthalenetetracarboxylic acid dianhydride and isolated as a deep blue waxy material[17] in an overall yield of 34%. The NDI core was substituted by secondary amines and further connected to trialkoxybenzamide (TB) wedges to promote H-bonding (among the amides) driven π-stacking. The control NDI derivative (**cNDI-2**) that is devoid of the structure-directing TB-wedge[18] was also prepared following a similar procedure (Scheme S1†).

UV/vis absorption studies reveal strong solvent effects on self-assembly of **cNDI-1**. In a "good" solvent such as $CHCl_3$ or THF, sharp absorption bands are noticed (Fig. 1a) at 353 and 370 nm (S_0–S_1) due to π–π* transitions and also a broad charge transfer band at 600 nm.[6] In methylcyclohexane (MCH), the π–π* absorption bands exhibit a significant bathochromic shift of ~11.0 nm in contrast to the control **cNDI-2** which does not exhibit such solvent dependent spectral changes (Fig. S1a†). The oscillator strength of the lowest energy π–π* transition band in THF and MCH was estimated (see ESI† for details) to be 14.1 and 10, respectively. Furthermore, photoluminescence spectra show (Fig. 1b) sharp emission bands in MCH exhibiting a mirror-image-like symmetry with the absorption bands with a smaller Stokes shift (20 nm) compared to that in THF (Stokes shift ~34 nm) suggesting J-aggregation of **cNDI-1** in MCH.[19] Although the quantum yield of **cNDI-1** was found to be low in both solvents, in MCH it was marginally higher (0.153%) than THF (0.07%) corroborating with literature precedence on J-aggregation.[16,19] For the control **cNDI-2**, the values were almost identical in THF (0.07%) and MCH (0.09%). ^{1}H NMR studies (Fig. 1c) further support self-assembly. In $CDCl_3$, both **cNDI-1** and **cNDI-2** exhibit sharp peaks at ~8.4 ppm corresponding to the aromatic proton of the NDI ring while in a nonpolar medium (MCH–C_6D_6: 9 : 1), the peak disappears only for **cNDI-1** suggesting its very high relaxation time as a result of firm self-assembly. It may also be related to a line broadening as a consequence of strong inter-chromophoric interactions. However, for **cNDI-2**, only an upfield shift is noticed which can be attributed to mere solvent dielectric effects. Thus taking into account these observations, it is conceivable that the TB-wedge dictates the J-aggregation of **cNDI-1** possibly by synergistic H-bonding interactions among the amide groups which were directly verified by solvent dependent FT-IR studies. Fig. 2a shows selected regions of the FT-IR spectra of **cNDI-1** in MCH and THF. To avoid confusion in peak assignments FT-IR spectra of **cNDI-2** were also recorded which show (inset, Fig. 2a) the peak positions of the imide carbonyls marked with blue arrows, but they are not of concern in the context of H-bonding of amides. In addition to those, characteristic peaks are noticed at 3387 cm^{-1}, 1650 cm^{-1} and 1585 cm^{-1} (marked with red arrow) in THF solution of **cNDI-1** for the N–H stretch, C=O stretch and amide-II, respectively, of the amide group. These peaks show pronounced solvent effects and appear at 3250 cm^{-1}, 1625 cm^{-1} and 1575 cm^{-1}, respectively, providing unequivocal evidence in support of inter-molecular H-bonding among the neighboring amide groups in J-aggregated **cNDI-1**.[20] Interestingly in the presence

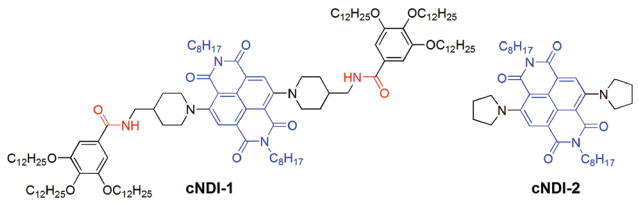

Scheme 1 Structure of the NDI building blocks.

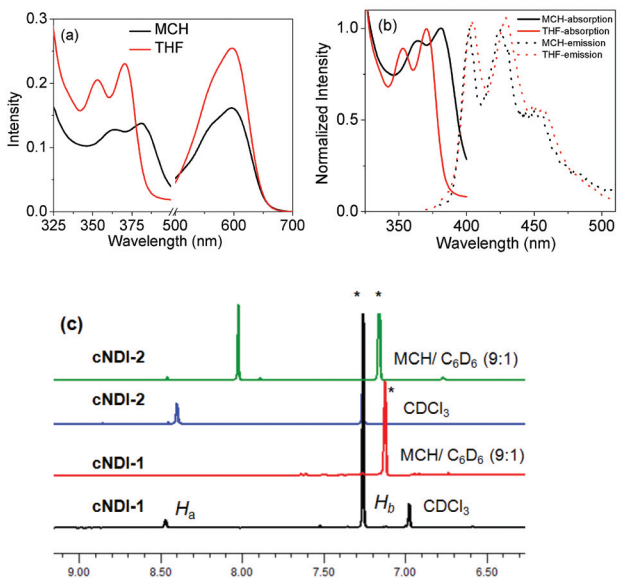

Fig. 1 (a) UV/Vis (l = 1.0 mm) and (b) intensity normalized absorption and emission (λ_{ex} = 350 nm) spectra of **cNDI-1** in THF and MCH. (c) ^{1}H NMR spectra (selected region) in $CDCl_3$ and MCH–C_6D_6 (9 : 1). *Indicates solvent peaks; C = 0.2 mM (UV), 2.0 mM (NMR); T = 25 °C. UV/Vis spectra of **cNDI-1** in benzene (Fig. S2†) do not reflect any specific interaction with the NDI chromophore and thus the presence of 10% C_6D_6 is not expected to cause any significant perturbation in the self-assembly process.

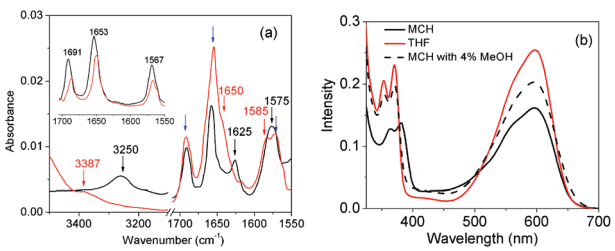

Fig. 2 (a) FT-IR spectra of **cNDI-1** (inset, **cNDI-2**) in THF (red line) and MCH (black line). C = 0.2 mM; T = 25 °C. (b) Effect of MeOH on the UV/vis spectra.

of even a trace amount of the H-bond competing solvent MeOH, the UV/vis spectrum of **cNDI-1** in MCH exhibits a significant blue shift (Fig. 2b) and almost resembles the monomeric spectrum in THF further ascertaining the decisive role of H-bonding on J-aggregation.

Solvent effects on macroscopic assembly and gelation

To understand the solvent effects on self-assembly, we compared the UV/Vis spectra of **cNDI-1** in a few other organic solvents (Fig. S2†) with varying polarity. In fact, apart from MCH, pronounced red-shifted spectra are observed only in *n*-decane which strongly favors H-bonding due to its low polarizability. However, **cNDI-1** shows a spontaneous macroscopic gelation[21,22] (for gelation test results in other solvents, see Table S1†) in *n*-decane (inset, Fig. 3b) with an entangled fibrillar structure (length: several micrometers, width: 30–40 nm) as revealed by high resolution transmission electron microscopy (HRTEM) images (Fig. 3b, S3†). In sharp contrast, spherical nanoparticles are seen (Fig. 3a, S3†) in the HRTEM images of **cNDI-1** in MCH and the solution does not turn to a gel (inset, Fig. 3a) even at a very high (10.0 mM) concentration. Atomic force microscopy (AFM) studies also suggest a similar contrast in morphology revealing spherical particles (width = 135 ± 15 nm, height = 12 ± 2 nm) and entangled fibers in MCH (Fig. 3c) and *n*-decane (Fig. 3d), respectively. However, virtually identical absorption and PL spectra (Fig. 3e) in *n*-decane and MCH confirm similar J-aggregation and MeOH-induced disassembly (Fig. S4†) confirms the involvement of H-bonding in both solvents. Similar changes in the ^{1}H NMR spectrum in decane (Fig. S5†) as observed in the case of MCH (Fig. 1c) suggest rigidification of the chromophore.

Thus, it becomes evident that the difference lies in the macroscopic assembly and not in the inter-chromophoric interaction. Furthermore, very similar spectral features in the gel state compared to a dilute solution in *n*-decane (Fig. 3f) suggest analogous inter-chromophoric interactions in the gel and the sol state. Then, why do such contrasting macroscopic structures exist in these two solvents of almost identical polarity? Powder X-ray diffraction (XRD) studies (Fig. 4b) provide valuable information to rationalize this intriguing observation. XRD data of the dried gel in *n*-decane show a sharp peak at $2\theta = 1.99°$ (d = 45 Å) nearly matching with the length of the **cNDI-1** along the *y*-direction (Fig. 4a) and also show successive peaks corresponding to $d/2$ and $d/3$ suggesting a lamellar packing. Interestingly, XRD patterns of a dried solution from MCH reveal an additional sharp peak at $2\theta = 5.3°$ (d = 16 Å). Such an intense peak is unlikely due to the $d/2$

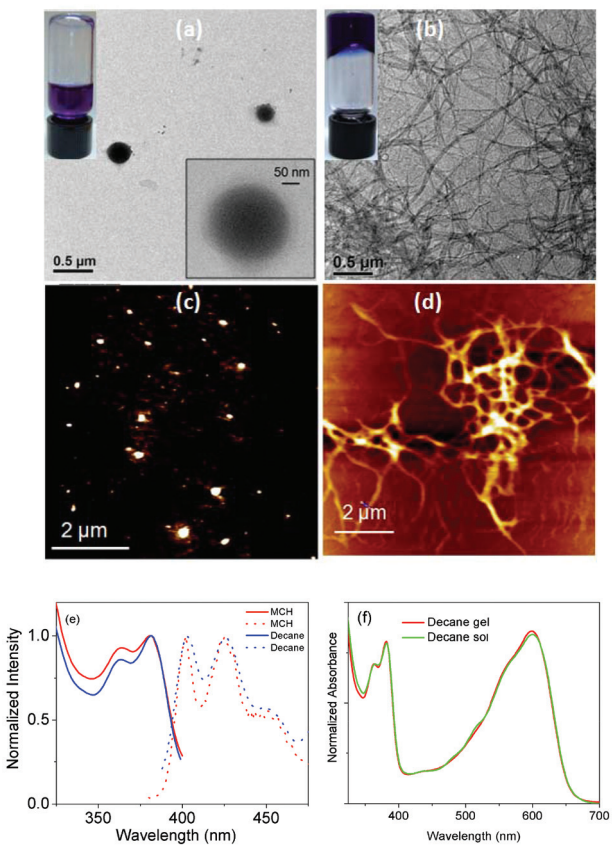

Fig. 3 HRTEM- (top) and AFM-images (bottom) of **cNDI-1** in MCH (a, c) and *n*-decane (b, d). Inset: images of **cNDI-1** solution and gel in MCH (a) and *n*-decane (b) at C = 4.0 mM; (e) normalized absorption and emission spectra of **cNDI-1** in MCH and *n*-decane (C = 0.2 mM, λ_{ex} = 350 nm); (f) normalized absorption spectra of **cNDI-1** in decane solution (C = 0.2 mM) and gel (C = 2.0 mM).

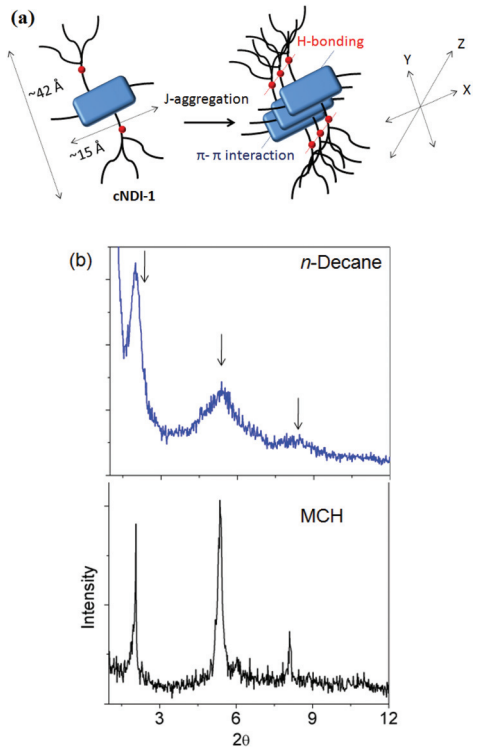

Fig. 4 (a) Proposed model for self-assembly; (b) XRD pattern of the dropcast sample from J-aggregated **cNDI-1** gel (*n*-decane) and sol (MCH).

(as in the case of *n*-decane). Interestingly, this distance matches closely with the length of the molecule along the *x*-direction. Thus, it appears that in MCH, the growth happens in all three directions by (H-bonding + π–π interactions), van der Waals interactions among the peripheral alkyl chains of the TB-wedge and C-8 chains connected to the imide position, which understandably leads to spherical structures as observed by HRTEM and AFM microscopy. However, in *n*-decane, the absence of an intense peak corresponding to the molecular length along the *x*-direction suggests no long range growth along this direction. This can be attributed to the capping of the C-8 chains by the linear hydrocarbon solvent molecules by effective van der Waals interactions. Thus instead of a 3D spherical structure, in this case fibrillar morphology is noticed.

To substantiate such possibility of a specific interaction of the extended C10 chains of *n*-decane with the alkyl chains[23] of the gelator, the possibility of external chiral induction[24] to the J-aggregated **cNDI-1** was examined by using two different chiral solvents, namely (*S*)-citronellyl bromide and (*S*)-limonene, which can be considered closely similar to *n*-decane and MCH, respectively, in terms of their linear and cyclic structures. The CD spectra of **cNDI-1** show (Fig. 5) intense bisignated Cotton effects in (*S*)-citronellyl bromide, but not in (*S*)-limonene. Interestingly, the CD band in (*S*)-citronellyl bromide disappears after the addition of trace amounts of trifluoroacetic acid as it destroys H-bonding and thus disrupts self-assembly. In fact, the chromophore itself does not contain any chiral centre and thus the observed Cotton effect has to be attributed to induction of chirality by the solvent molecules, which itself is only effective in the case of the straight chain chiral solvent due to a more efficient van der Waals interaction with the peripheral alkyl chains of the gelator.

In this scenario one can expect tunable gelation depending on the length of the hydrocarbon solvent, as this will determine the efficacy of interaction. To test this hypothesis, we studied gelation in *n*-hexane (C6), *n*-octane (C8), *n*-decane (C10) and *n*-dodecane (C12) solvents in which the gelation properties are indeed very different (Table 1). For instance, in *n*-dodecane a gel was formed within ~15 min, while it took ~18 h in *n*-hexane. This is also reflected in the viscoelastic properties of the gels as revealed by stress-amplitude sweep measurements in different solvents. At a lower value of applied stress, storage modulus (G') > loss modulus (G'') is observed (Table 1) for all samples suggesting the existence of a typical gel phase. The value of G'–G'' which indicates that the elastic nature shows almost one order of magnitude increase for the *n*-dodecane gel compared to the *n*-hexane gel (Fig. 6), while the values in the *n*-octane and *n*-decane gel (Fig. S6†) lie in-between (Table 1).

Furthermore, the yield-stress (σ_y) (the critical value where G' becomes less than G''), a parameter that indicates robustness, also follows the same trend confirming this unprecedented impact of the chain length of the aliphatic hydrocarbon solvents on gelation. It is noteworthy that the solubility parameters of these solvents[25] are almost comparable and slightly increases (Table S2†) with increasing chain length. Thus as per literature precedence[26] the CGC should have increased going from *n*-hexane to *n*-dodecane, but we noticed the opposite trend. Furthermore the solubility parameters of MCH and *n*-dodecane are almost the same (Table S2†) but we find no gelation in MCH while strongest gelation in *n*-dodecane. Thus the solvent dependent gelation in the present system cannot be rationalized based on mere solubility parameters of the solvents. Intriguingly the absorption spectra of **cNDI-1**, measured soon after solution preparation, look almost identical (Fig. S7†) in all cases, indicating spontaneous J-aggregation irrespective of the chain length of the solvent molecules. The question arises as to why gelation is so slow? To answer this question, we examined the morphology of **cNDI-1** in *n*-octane by AFM microscopy at different time intervals (Fig. 7) which shows a very interesting morphology evolution during aging.[27] For a freshly prepared solution, spherical particles are noticed even in this case (like in MCH) which gradually convert to

Table 1 Solvent effects on gelation of **cNDI-1** (C = 4.0 mM)

Properties	*n*-Hexane	*n*-Octane	*n*-Decane	*n*-Dodecane
Time (min)	1100	480	60	15
T_g/°C	38	46	64	76
CGC (mM)	2.8	2.0	1.2	0.8
G' (Pa)	38	74	92	794
G'' (Pa)	8.0	10	13	88
σ_y (Pa)	0.2	1.0	1.7	4.9

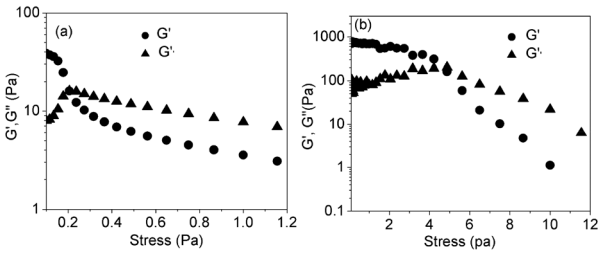

Fig. 6 Stress amplitude sweep measurements results for **cNDI-1** gel (C = 10 mM) in (a) *n*-hexane and (b) *n*-dodecane.

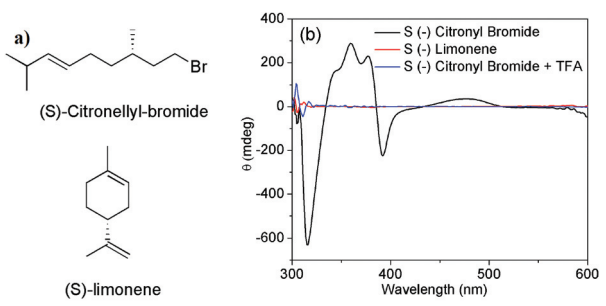

Fig. 5 Solvent dependent CD spectra of **cNDI-1**. The chemical structures of the solvents are shown on the left.

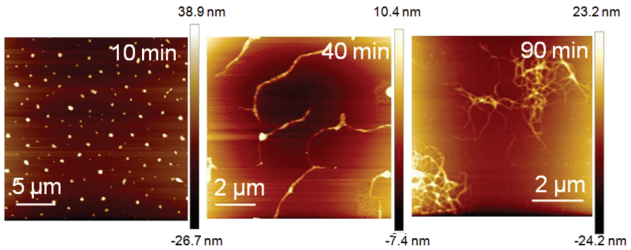

Fig. 7 AFM-images of **cNDI-1** in *n*-octane at different times. The time indicated in each image represents the aging time after which the solution was drop-casted for AFM imaging. But as imaging was done after drying the drop-casted sample, the morphology observed may not be exactly identical to those in solution after the same time interval.

fibrils leading to gelation as a result of van der Waals interactions between solvent molecules and the alkyl chains of the gelator. It is conceivable that the efficacy of such an interaction increases with the length of the alkyl chain which eventually determines the time required for gelation and in addition the physical properties of the gels (Table 1). On the other hand, cyclic hydrocarbons such as MCH or cyclohexane, lacking such propensity to interact with the alkyl chains of the gelator, are unable to produce a macroscopic gel, even though similar J-aggregation was noticed.

Impact of J-aggregation on excited state dynamics

Finally, we performed ultrafast transient absorption pump–probe spectroscopy to elucidate the excited state dynamics of **cNDI-1** in different solvents on the picosecond to nanosecond timescale as depicted in Fig. 8 and 9. The measurements reveal a strong dependence of the excited state lifetimes on the polarity of the solvent. THF was used as a "good" solvent, in which mainly monomeric states of **cNDI-1** exist (Fig. 1). The transient spectra after 1 ps shown in Fig. 8a exhibit a ground-state bleach (GSB) originating from the depopulation of the ground state at the position of the charge transfer absorption band and moreover photo-induced absorption (PIA) features below 558 nm and above 688 nm. The spectral features remain virtually the same after 1 ps. However, on the sub-ps timescale we observed spectral changes (Fig. 9) indicating the transition from the primary photoexcitation to an intramolecular charge-transfer (CT) state.

This implies ultrafast electron transfer from the electron rich amine wedge to the NDI core within the temporal resolution of our TA setup of ~200 fs. The ps–ns decay dynamics of the PIA peak around 750 nm is shown in Fig. 8b (open symbols). The excited state decay in THF can be described by a biexponential function consisting of a short-lived component with an inverse decay rate of 6.6 ps and a relative amplitude of 70% and a longer-lived component exhibiting an inverse decay rate of 44 ps with a relative amplitude of 30%. We assign the short component to a fast decay of excited states, while the slow component is assigned to the recombination of intramolecular CT states. This is in line with previous reports, for

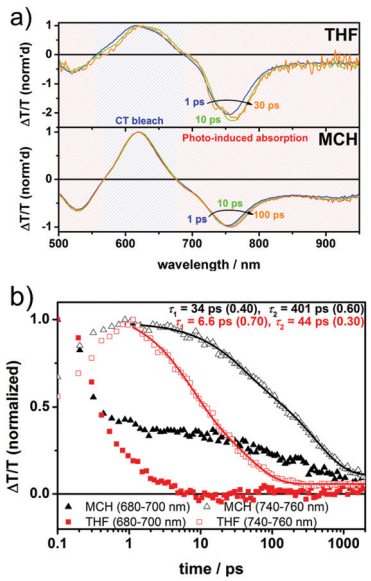

Fig. 8 (a) Picosecond transient absorption spectra of **cNDI-1** in THF (upper panel) and MCH (lower panel) and (b) kinetics of the bleach and photoinduced absorption in THF (red squares) and MCH (black triangles) tracked between 680–700 nm (filled symbols) and 740–760 nm (open symbols).

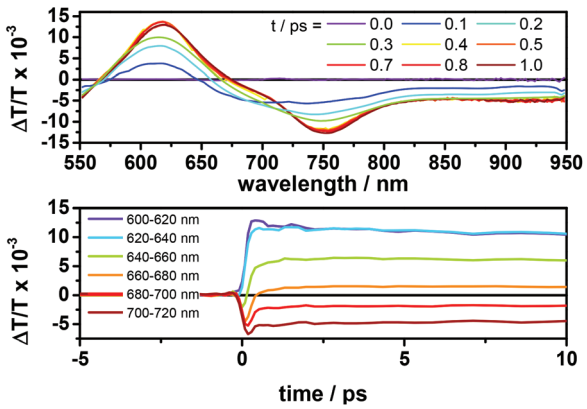

Fig. 9 Sub-ps spectra of **cNDI-1** in MCH (upper panel) and dynamics at various wavelength regions (lower panel).

instance, such decay dynamics on the timescale of tens of picoseconds have been reported earlier for nitrogen-substituted NDIs.[28] **cNDI-1** was also measured in MCH in which it shows J-aggregation. MCH was particularly chosen as the solvent for TA experiments as it avoids scattering of pump and probe beams on the one hand, while maintaining a sufficient degree of supramolecular organization on the other hand. **cNDI-1** excited states exhibit distinct differences in MCH compared to THF. Interestingly, the ratio of the peaks of GSB and PIA is altered. While the measurement in THF resulted in a peak ratio of GSB : PIA ~ 1 : 2, it was only 1 : 1 in MCH. The PIA peak at 750 nm is assigned to NDI anions according to the

literature.[9] We note, that a similar change has been reported for perylenediimide (PDI) derivatives.[29] We speculate that the higher NDI anion absorption in THF can be explained by a stronger localization of the charge on a single chromophore unit resulting in a more pronounced charge-induced absorption peak. In contrast, in MCH delocalization is enabled by aggregation and therefore the relative intensity of the spectral feature is reduced. Furthermore, a feature around 900 nm evolves, which is assigned to aggregates, as previously also observed for PDI derivatives. In line with the spectral changes, a prolongation of excited state lifetimes was observed. A biexponential fit to the decay dynamics obtained from TA measurements in MCH yielded inverse decay rates of 34 ps and 401 ps with relative amplitudes of 40% and 60%, respectively. The considerable extension of the excited state lifetime by more than one order of magnitude is likely caused by an increased separation of charges enabled by the aggregation of chromophores and hence an increased delocalization[30] of charge separated states.

Conclusions

In summary, we have demonstrated for the first time the design of a supramolecular building block based on an amine-substituted NDI-chromophore for H-bonding driven J-aggregation in non-polar solvents and its effect on excited state dynamics. Unprecedentedly, the lifetime of the charge-separated state could be prolonged by more than one order of magnitude by J-aggregation, which appears highly promising for various applications including efficient photo-catalysis and energy conversion.[31,32] We have also shown intriguing solvent effects on self-assembly. While the polarity, which influences H-bonding, dictated the J-aggregation, the macroscopic structure and gelation showed a strong dependence on the structure of the solvent molecules. Linear and cyclic hydrocarbons produced contrasting morphologies (fibrillar and spherical, respectively), leading to macroscopic gelation only in the former cases. While several reports have correlated solvent effects on gelation[33] by different physical parameters such as Hildebrand, Hansen and Kamlet–Taft parameters, polarity ($E_t(30)$) or dielectric constant, this is the first example to the best of our knowledge demonstrating that even a variation in the chain length or structure, namely linear *vs.* cyclic, in a series of aliphatic hydrocarbon solvents with identical polarity can impose such a remarkable influence on morphology.

Acknowledgements

HK thanks CSIR, India for a research fellowship. SG thanks SERB, India for funding (Project no: SR/S1/OC-18/2012). FL thanks the Max Planck Society for funding the Max Planck Research Group and gratefully acknowledges a Kekulé scholarship of the Fonds der Chemischen Industrie (FCI).

Notes and references

1 F. J. M. Hoeben, P. Jonkheijm, E. W. Meijer and A. P. H. J. Schenning, *Chem. Rev.*, 2005, **105**, 1491; Z. Chen, A. Lohr, C. R. Saha-Möller and F. Würthner, *Chem. Soc. Rev.*, 2009, **38**, 564; T. Nakanishi, *Chem. Commun.*, 2010, **46**, 3425; T. F. A. De Greef, M. M. J. Smulders, M. Wolffs, A. P. H. J. Schenning, R. P. Sijbesma and E. W. Meijer, *Chem. Rev.*, 2009, **109**, 5687; A. Ajayaghosh and V. K. Praveen, *Acc. Chem. Res.*, 2007, **40**, 644; S. Yagai and A. Kitamura, *Chem. Soc. Rev.*, 2008, **37**, 1520; A. Mishra, C.-Q. Ma and P. Bauerle, *Chem. Rev.*, 2009, **109**, 1141; D. G. Rodríguez and A. P. H. J. Schenning, *Chem. Mater.*, 2011, **23**, 310; F. Würthner, *Chem. Commun.*, 2004, 1564; M. R. Molla and S. Ghosh, *Phys. Chem. Chem. Phys.*, 2014, **16**, 26672; A. Das and S. Ghosh, *Angew. Chem., Int. Ed.*, 2014, **53**, 2038.

2 L. Magginia and D. Bonifazi, *Chem. Soc. Rev.*, 2012, **41**, 211; S. S. Babu, S. Prasanthkumar and A. Ajayaghosh, *Angew. Chem., Int. Ed.*, 2012, **51**, 1766.

3 A. Saeki, Y. Koizumi, T. Aida and S. Seki, *Acc. Chem. Res.*, 2012, **45**, 1193.

4 A. W. Hains, Z. Liang, M. A. Woodhouse and B. A. Gregg, *Chem. Rev.*, 2010, **110**, 6689; J. Mei, Y. Diao, A. L. Appleton, L. Fang and Z. Bao, *J. Am. Chem. Soc.*, 2013, **135**, 6724.

5 For a review on supramolecular biomaterials see: K. P. Milroy, M. H. Sonntag and L. Brunsveld, *Chem. – Eur. J.*, 2013, **19**, 10786.

6 For a review on cNDI see: N. Sakai, J. Mareda, E. Vauthey and S. Matile, *Chem. Commun.*, 2010, **46**, 4225.

7 For representative examples on cNDI based organic materials see: T. Earmme, Y.-J. Hwang, N. M. Murari, S. Subramaniyan and S. A. Jenekhe, *J. Am. Chem. Soc.*, 2013, **135**, 14960; B. C. Popere, A. M. Della Pelle and S. Thayumanavan, *Macromolecules*, 2011, **44**, 4767; B. A. Jones, A. Facchetti, T. J. Marks and M. R. Wasielewski, *Chem. Mater.*, 2007, **19**, 2703; J. H. Oh, S.-L. Suraru, W.-Y. Lee, M. Könemann, H. W. Höffken, C. Röger, R. Schmidt, Y. Chung, W.-C. Chen, F. Würthner and Z. Bao, *Adv. Funct. Mater.*, 2010, **20**, 2148; R. Bhosale, R. S. K. Kishore, V. Ravikumar, O. Kel, E. Vauthey, N. Sakai and S. Matile, *Chem. Sci.*, 2010, **1**, 357; K. Baeg, D. Khim, S. Jung, M. Kang, I. You, D. Kim, A. Facchetti and Y. Noh, *Adv. Mater.*, 2012, **24**, 5433; Y. A. Getmanenko, S. Singh, B. Sandhu, C. Wang, T. Timofeeva, B. Kippelen and S. R. Marder, *J. Mater. Chem. C*, 2014, **2**, 124; C. Röger, Y. Miloslavina, D. Brunner, A. R. Holzwarth and F. Würthner, *J. Am. Chem. Soc.*, 2008, **130**, 5929; S. Bevers, S. Schutte and L. W. McLaughlin, *J. Am. Chem. Soc.*, 2000, **122**, 5905; S. Chopin, F. Chaignon, E. Blart and F. Odobel, *J. Mater. Chem.*, 2007, **17**, 4139; R. Fernando, Z. Mao, E. Muller, F. Ruan and G. Sauvé, *J. Phys. Chem. C*, 2014, **118**, 3433.

8 For a review on conjugated polymers based on NDI see: J. Wang and T. Higashihara, *Polym. Chem.*, 2013, **4**, 5518.

9 S. V. Bhosale, C. H. Jani and S. J. Langford, *Chem. Soc. Rev.*, 2008, **37**, 331.

10 P. Mukhopadhyay, Y. Iwashita, M. Shirakawa, S.-i. Kawano, N. Fujita and S. Shinkai, *Angew. Chem., Int. Ed.*, 2006, **45**, 1592; G. D. Pantos, P. Pengo and J. K. M. Sanders, *Angew. Chem., Int. Ed.*, 2007, **46**, 194; J. Zheng, W. Qiao, X. Wan, J. P. Gao and Z. Y. Wang, *Chem. Mater.*, 2008, **20**, 6163; H. Shao and J. R. Parquette, *Chem. Commun.*, 2010, **46**, 4285; S. Tu, S. H. Kim, J. Joseph, D. A. Modarelli and J. R. Parquette, *J. Am. Chem. Soc.*, 2011, **133**, 19125; M. Kumar and S. J. George, *Chem. Sci.*, 2014, **5**, 3025; M. B. Avinash, E. Verheggen, C. Schmuck and T. Govindaraju, *Angew. Chem., Int. Ed.*, 2012, **51**, 10324.

11 In the past few years we have reported various supramolecular strategies for H-bonding driven self-assembly of NDI-building blocks in organic and water media and also in macromolecular systems. For representative examples see: M. R. Molla and S. Ghosh, *Chem. Mater.*, 2011, **23**, 95; M. R. Molla and S. Ghosh, *Chem. – Eur. J.*, 2012, **18**, 9849; A. Das and S. Ghosh, *Macromolecules*, 2013, **46**, 3939; A. Das and S. Ghosh, *Angew. Chem., Int. Ed.*, 2014, **53**, 1092.

12 I. D. Cat, C. Röger, C. C. Lee, F. J. M. Hoeben, M. J. Pouderoijen, A. P. H. J. Schenning, F. Würthner and S. De Feyter, *Chem. Commun.*, 2008, 5496; S. V. Bhosale, C. Jani, C. H. Lalander and S. J. Langford, *Chem. Commun.*, 2010, **46**, 973; S. V. Bhosale, C. H. Jani, C. H. Lalander, S. J. Langford, I. Nerush, J. G. Shapter, D. Villamaina and E. Vauthey, *Chem. Commun.*, 2011, 8226.

13 S.-L. Suraru and F. Würthner, *Angew. Chem., Int. Ed.*, 2014, **53**, 7428.

14 S. S. Babu, K. K. Kartha and A. Ajayaghosh, *J. Phys. Chem. Lett.*, 2010, **1**, 3413.

15 S. Bhosale, A. L. Sisson, P. Talukdar, A. Fürstenberg, N. Banerji, E. Vauthey, G. Bollot, J. Mareda, C. Röger, F. Würthner, N. Sakai and S. Matile, *Science*, 2006, **313**, 84.

16 For a recent review on J-aggregation see: F. Würthner, T. E. Kaiser and C. R. Saha-Möller, *Angew. Chem., Int. Ed.*, 2011, **50**, 3376.

17 The waxy nature of such a high molecular weight material although can be counterintuitive but recent reports suggest that alkyl chain crowding may induce such amorphous nature even for pi-conjugated systems. For details see: S. S. Babu, M. J. Hollamby, J. Aimi, H. Ozawa, A. Saeki, S. Seki, K. Kobayashi, K. Hagiwara, M. Yoshizawa, H. Möhwald and T. Nakanishi, *Nat. Commun.*, 2013, **4**, 1969–1961.

18 H. Kar, M. R. Molla and S. Ghosh, *Chem. Commun.*, 2013, **49**, 4220.

19 For very similar spectral changes in the case of J-aggregating perylene dyes see: X.-Q. Li, X. Zhang, S. Ghosh and F. Würthner, *Chem. – Eur. J.*, 2008, **14**, 8074. For examples on J-aggregation of unsubstituted NDI see: H. Shao, T. Nguyen, N. C. Romano, D. A. Modarelli and J. R. Parquette, *J. Am. Chem. Soc.*, 2009, **131**, 16374; M. R. Molla, D. Gehrig, L. Roy, V. Kamm, A. Paul, F. Laquai and S. Ghosh, *Chem. – Eur. J.*, 2014, **20**, 760; S. Choi, J. Bouffard and Y. Kim, *Chem. Sci.*, 2014, **5**, 751.

20 S. Cantekin, T. F. A. de Greefab and A. R. A. Palmans, *Chem. Soc. Rev.*, 2012, **41**, 6125; S. Diring, F. Camerel, B. Donnio, T. Dintzer, S. Toffanin, R. Capelli, M. Muccini and R. Ziessel, *J. Am. Chem. Soc.*, 2009, **131**, 18177.

21 For a recent review on pi-gelators see: S. S. Babu, V. K. Praveen and A. Ajayaghosh, *Chem. Rev.*, 2014, **114**, 1973.

22 For general reviews on small molecule gelators see: L. A. Estroff and A. D. Hamilton, *Chem. Rev.*, 2004, **104**, 1201; N. M. Sangeetha and U. Maitra, *Chem. Soc. Rev.*, 2005, **34**, 821; L. E. Buerkle and S. J. Rowan, *Chem. Soc. Rev.*, 2012, **41**, 6089.

23 M. J. Hollamby, M. Karny, P. H. H. Bomans, N. A. J. M. Sommerdijk, A. Saeki, S. Seki, H. Minamikawa, I. Grillo, B. R. Pauw, P. Brown, J. Eastoe, H. Möhwald and T. Nakanishi, *Nat. Chem.*, 2014, **6**, 690.

24 For representative examples on chiral induction see: E. Yashima and K. Maeda, *Macromolecules*, 2008, **41**, 3; H. Goto, Y. Okamoto and E. Yashima, *Macromolecules*, 2002, **35**, 4590; L. Brunsveld, J. A. J. M. Vekemans, J. H. K. K. Hirschberg, R. P. Sijbesma and E. W. Meijer, *Proc. Natl. Acad. Sci. U. S. A.*, 2002, **99**, 4977; A. P. H. J. Schenning, J. v. Herrikhuyzen, P. Jonkheijm, Z. Chen, F. Würthner and E. W. Meijer, *J. Am. Chem. Soc.*, 2002, **124**, 10252; M. R. Molla, A. Das and S. Ghosh, *Chem. Commun.*, 2011, **47**, 8934.

25 A. F. M. Barton, *Chem. Rev.*, 1975, **75**, 731.

26 K. Hanabusa, M. Matsumoto, M. Kimura, A. Kakehi and H. Shirai, *J. Colloid Interface Sci.*, 2000, **224**, 231.

27 A. Das, B. Maity, D. Koley and S. Ghosh, *Chem. Commun.*, 2013, 5757; C. Rest, A. Martin, V. Stepanenko, N. K. Allampally, D. Schmidt and G. Fernández, *Chem. Commun.*, 2014, **50**, 13366.

28 U. Megerle, I. Pugliesi, C. Schriever, C. F. Sailer and E. Riedle, *Appl Phys B: Lasers Opt.*, 2009, **96**, 215; I. Pugliesi, U. Megerle, S.-L. Suraru, F. Würthner, E. Riedle and S. Lochbrunner, *Chem. Phys. Lett.*, 2011, **504**, 24; S. Chopin, F. Chaignon, E. Blart and F. Odobel, *J. Mater. Chem.*, 2007, **17**, 4139.

29 J. M. Lim, P. Kim, M. Yoon, J. Sung, V. Dehm, Z. Chen, F. Würthner and D. Kim, *Chem. Sci.*, 2013, **4**, 388.

30 For recent reports on delocalization effects on the NDI radical anion see: A. Takai, T. Yasuda, T. Ishizuka, T. Kojima and M. Takeuchi, *Angew. Chem., Int. Ed.*, 2013, **52**, 9167; Y. Wu, M. Frasconi, D. M. Gardner, P. R. McGonigal, S. T. Schneebeli, M. R. Wasielewski and J. F. Stoddart, *Angew. Chem., Int. Ed.*, 2014, **53**, 9476.

31 S. Fukuzumi, *Electron Transfer of p-Functional Systems and Applications, Functional Organic Materials*, Wiley-VCH, 2007, pp. 465–510.

32 For a very recent report on visible light induced catalysis using perylene dyes, see: I. Ghosh, T. Ghosh, J. I. Bardagi and B. König, *Science*, 2014, **346**, 725.

33 P. Curcio, F. Allix, G. Pickaert and B. J. Grégoire, *Chem. – Eur. J.*, 2011, **17**, 13603; A. R. Hirst and D. K. Smith, *Langmuir*, 2004, **20**, 10851; W. Edwards, C. A. Lagadec and D. K. Smith, *Soft Matter*, 2011, **7**, 110; Y. Jeong, K. Hanabusa, H. Masunaga, I. Akiba, K. Miyoshi, S. Sakurai and K. Sakurai, *Langmuir*, 2005, **21**, 586; P. Zhu, X. Yan, Y. Su, Y. Yang and J. Le, *Chem. – Eur. J.*, 2010, **16**, 3176; T. Pinault, B. Isare and L. Bouteiller, *ChemPhysChem*, 2006, **7**, 816; A. Aggeli, M. Bell, N. Boden, J. N. Keen, P. F. Knowles, T. C. B. McLeish, M. Pitkeathly and S. E. Radford, *Nature*, 1997, **386**, 259.